Antibody Colocalization Microarray: A Scalable Technology for Multiplex Protein Analysis in Complex Samples*[S]

M. Pla-Roca‡§, R. F. Leulmi‡§, S. Tourekhanova‡§, S. Bergeron‡§, V. Laforte‡§¶, E. Moreau‡§, S. J. C. Gosline‖, N. Bertos‖‡‡, M. Hallett‖**, M. Park‖‡‡§§¶¶, and D. Juncker‡§¶‖‖**

DNA microarrays were rapidly scaled up from 256 to 6.5 million targets, and although antibody microarrays were proposed earlier, sensitive multiplex sandwich assays have only been scaled up to a few tens of targets. Cross-reactivity, arising because detection antibodies are mixed, is a known weakness of multiplex sandwich assays that is mitigated by lengthy optimization. Here, we introduce (1) *vulnerability* as a metric for assays. The vulnerability of multiplex sandwich assays to cross-reactivity increases quadratically with the number of targets, and together with experimental results, substantiates that scaling up of multiplex sandwich assays is unfeasible. We propose (2) a novel concept for multiplexing without mixing named antibody colocalization microarray (ACM). In ACMs, both capture and detection antibodies are physically colocalized by spotting to the same two-dimensional coordinate. Following spotting of the capture antibodies, the chip is removed from the arrayer, incubated with the sample, placed back onto the arrayer and then spotted with the detection antibodies. ACMs with up to 50 targets were produced, along with a binding curve for each protein. The ACM was validated by comparing it to ELISA and to a small-scale, conventional multiplex sandwich assay (MSA). Using ACMs, proteins in the serum of breast cancer patients and healthy controls were quantified, and six candidate biomarkers identified. Our results indicate that ACMs are sensitive, robust, and scalable. ***Molecular & Cellular Proteomics 11: 10.1074/mcp.M111.011460, 1–12, 2012.***

From the ‡Biomedical Engineering Department, §McGill University and Genome Quebec Innovation Centre, ¶Department of Neurology and Neurosurgery, McGill University, 740 Dr. Penfield Avenue, H3A 1A4, Montreal, Quebec, Canada; ‖Rosalind and Morris Goodman Cancer Research Centre, 1160 Pine Ave. West, H3A 1A3 Montreal, Quebec, Canada; **McGill Centre for Bioinformatics, School of Computer Science, McGill University, 3649 Promenade Sir William Osler, H3A 0B1, Quebec, Canada; ‡‡Department of Medicine, and §§Departments of Biochemistry and Oncology, McGill University, Montreal, H3G 1Y6; ¶¶Department of Medicine, McGill University Health Center, Montreal

Received May 30, 2011, and in revised form, November 10, 2011
⌘ *Author's Choice*—Final version full access.
Published, MCP Papers in Press, December 14, 2011, DOI 10.1074/mcp.M111.011460

Semiconductors are the paradigm for scalable technologies. These grew exponentially over four decades by doubling the density of elements and processing speed roughly every two years following Moore's law (1). DNA microarrays, introduced in the early nineties, were also scalable and expanded from initially 256 (2) to 6.5 million probes per chip (3) in about 10 years. DNA chips were rapidly adopted and helped transform our understanding of biology of healthy organisms (4) and of disease (5, 6). Despite initial reliability issues (7), they were subsequently adopted for clinical use. Although multiplexing and miniaturization of protein assays as a microarray were proposed by Ekins *et al.* (8) in 1989, well before DNA microarrays, multiple challenges have delayed its scaling up and widespread adoption. As in DNA microarrays, sample labeling can be used to reveal binding of analytes to each spot. Direct labeling facilitates scaling of the number of targets on an array (9), or on beads (10), as only a single Ab is required per analyte. Sample labeling can also be avoided altogether when label-free biosensors are used (11). However, cross-reactivity and heterogeneous labeling of proteins both limit the sensitivity and robustness of direct assays comparatively to sandwich assays described below. High sensitivity is important to many applications, and, for example, the detection of cancer proteins secreted by tumors into blood is very challenging owing to their high dilution and very low concentration, (12) as well as masking by highly abundant proteins (13). Whereas direct labeling has been successfully used to identify biomarkers for cancer prognosis for example (14), the specificity and reliability of this approach has been questioned (15). Masse spectrometry (MS)[1] can be used for multiplex protein analysis and although it is intrinsically biased toward high abundance proteins, significant progress has been made recently. In 2009, a large scale study showed a limit of detection (LOD) of $\sim$2 μg/ml (16), and since then significant progress was made and two studies have now successfully established a biomarker validation pipelines for

[1] The abbreviations used are: MS, Mass spectrometry; LOD, limit of detection; MSA, multiplex sandwich assay; ACM, antibody colocalization microarray; Ab, antibody; cAb, capture antibody; dAb, detection antibody; SA, streptavidin; PBS, phosphate buffered saline.

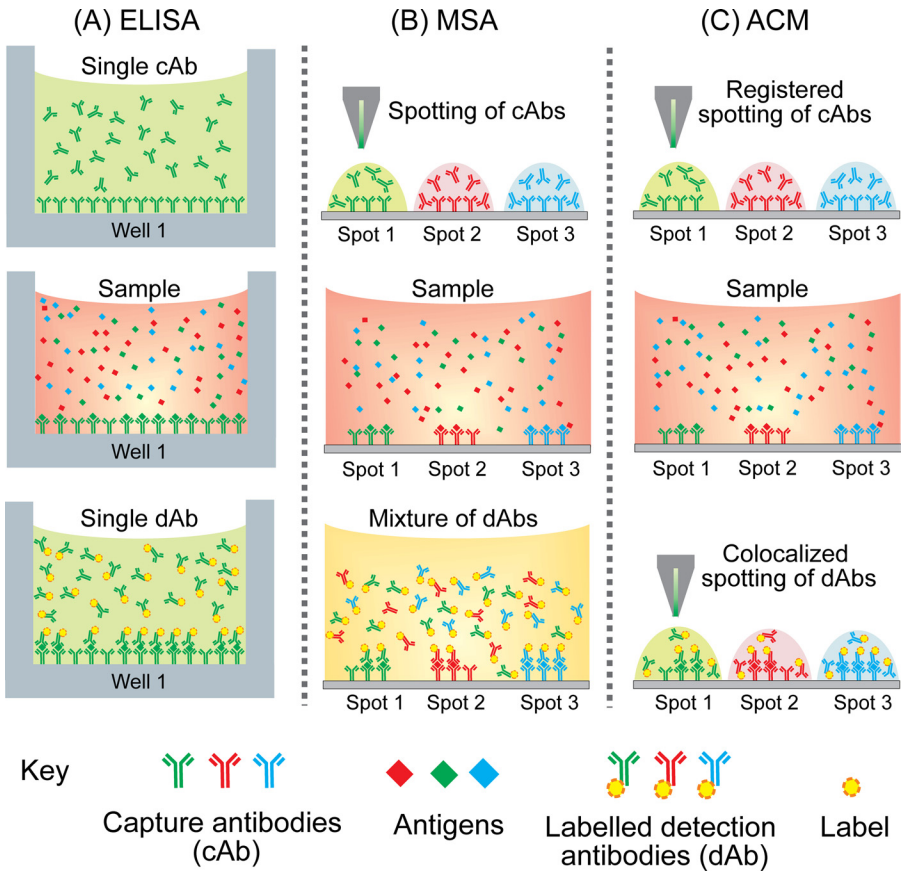

FIG. 1. **Schematic process flow for three sandwich assay formats, namely the ELISA (a singleplex assay), multiplexed sandwich assays (MSA) in microarray format, and the antibody colocalization microarray (ACM).** *A*, In the ELISA, a single well is coated with a cAb, incubated with a sample, and following rinsing, a single, matched dAb incubated for detection. The dual binding of two Abs to a single analyte confers tolerance to cross-reactivity and nonspecific binding. *B*, In an MSA, cAbs are arrayed on a slide, which is incubated with a sample, and after rinsing, with a mixture of dAbs. *C*, In an ACM, the initial steps are identical to a MSA, with the difference that the first spotting is precisely registered and that a second round of spotting is used to deliver each dAb exactly on the spots with the matched cAb, physically colocalizing them. This protocol avoids mixing of reagents, and ACM may be seen as an array of singleplex nano-sandwich assays, each requiring only ~ 1 nL of dAb solution.

detection of proteins in the ng/ml range in plasma (17, 18). These results validate MS for identifying biomarkers across the human proteome, but both pipelines required (i) using multiple MS instruments and advanced protocols, (ii) weeks and months of instrument time for data acquisition, (iii) depletion of abundant proteins in the plasma, which is labor intensive and may result in loss of biomarker proteins, and (iv) high concentrations of the candidate biomarkers in the sample for the first step of the validation pipeline, which may not be practical for some diseases.

The sandwich immunoassay (Fig. 1*A*), which is widely used for enzyme-linked immunosorbent assays (ELISAs), is the "gold standard" for detecting proteins at low concentrations. Sandwich immunoassays, in contrast to direct labeling assays, are tolerant to cross-reactivity, which does not necessarily lead to false positive signals or noise. The dual binding of capture (cAb) and detection antibody (dAb) to two different epitopes of the same protein prevents a single cross-reaction, or the nonspecific binding of a protein to a spot, from generating a false positive signal because the dAb will not bind. Sandwich assays have been continuously improved and single molecules can now be detected (19), but in samples with complex matrices such as blood, "interference" still occurs and the LOD in clinical tests is limited to high femtomolar (<1 pg/ml) concentrations for the best antibodies available (20).

Multiplex protein profiling can be performed using multiplexed sandwich assays (MSAs). However, in MSAs, dAbs are applied as a mixture (Fig. 1*B*), which causes them to interact with each other, the cAbs, and any other molecule immobilized on any of the spots. Cross-reactivity among reagents, notably nonmatched pairs of Abs, will inevitably produce a false positive signal and background noise. This issue has long been recognized (21), but mixing has been considered inherent to MSAs up to now (22), and an important step in the design of microarrays and bead-based MSAs is systematic, combinatorial testing for cross-reactivity between each Ab and all other Abs and analytes, one by one. This costly and labor-intensive process has been described in detail (23, 24). Kingsmore and colleagues set the practical limit for multiplexing to 30–50 targets (23), and indeed, current MSAs have not been scaled beyond this limit (23–27). However, even this limit could only be reached with arrays primarily targeting cytokines, where libraries of high quality Abs are available (23, 28). For many proteins, notably novel candidate biomarkers, there is a lack of Abs, thus severely limiting the level of multiplexing in MSAs, and often requiring separate assays for particular analytes (25, 29).

Here, we introduce vulnerability to cross-reactivity as a novel metric and establish the scaling law for MSA vulnerability as a function of the number of targets. Next, we experimentally illustrate that even for a moderate number of targets,

cross-reactivity is widespread. We propose a conceptually different approach to multiplexing called the antibody colocalization microarray (ACM) that eliminates mixing of reagents and vulnerability to cross-reactions by spotting each cAb and each matched dAb precisely onto the same spot (Fig. 1*C*). We establish a multiplexed ACM with 50 proteins and compare it to conventional multiplex assays with low multiplexing. We profile proteins in the blood of 15 breast cancer patients and 11 healthy controls, and identify six candidate biomarkers. The results confirm the potential of ACM for multiplexed analysis in complex samples and demonstrate that this technology can be scaled up without compromising assay robustness and performance.

EXPERIMENTAL PROCEDURES

Customized Microarrayer—The antibodies were arrayed using a customized Nanoplotter 2.1 microarrayer (GeSiM (Gesellschaft fuer Silizium-Mikrosysteme GmbH), Grosserkmannsdorf, Germany) equipped with a silicon contact pin printing head (Parallel Synthesis, Santa Clara, CA), a precision microfabricated silicon collimator (Parallel Synthesis), and a customized slide tray with individual spring-loaded clamps for each slide (GeSIM) (supplementary Fig. S1).

Antibodies and Analytes—Both the matched antibody pairs and their protein markers were purchased from the same supplier source. All the dAbs were purchased in biotinylated form, except for CA15–3 that was biotinylated in our laboratory using the Biotin-XX Microscale Protein Labeling Kit (Invitrogen, Carlsbad, CA). Labeled streptavidin Cy-5 was obtained from Rockland Immunochemicals (Gilbertsville, PA).Green fluorescent protein (GFP) (Rockland Immunochemicals, Gilbertsville, PA) was used as an internal calibrator. All antibodies and recombinant proteins were reconstituted and stored according to the supplier's instructions. The list of antibodies and recombinant proteins can be found in supplementary Table S1.

Buffers—Dilution Buffer (PBST): 0.1% Tween-20 (Sigma-Aldrich) in PBS (Fisher Scientific, Nepean, ON). Blocking buffer: BSA-Free StabilGuard® Choice Microarray Stabilizer (SurModics, Eden Praire, MN) (used as provided by the supplier). Detection antibody spotting buffer: 30% glycerol (Sigma-Aldrich) in BSA-Free StabilGuard® Choice Microarray Stabilizer (SurModics). cAb spotting buffer: 30% Glycerol in PBST.

Microarray Fabrication—The cAbs were diluted in cAb spotting buffer (supplementary Table S1 online lists the different concentrations used). Multiple spotting rounds with different Abs were carried out to form the array microscope slides with 16 nitrocellulose pads (ONCYTE Avid slides, Grace Biolabs, Bend, OR). The humidity during the printing procedures was adjusted to 50 and 75% for cAbs and dAbs, respectively, in order to minimize evaporation of solutions while printing. The silicon pins had a 75 μm $\times$ 75 μm foot print giving a spot size of $\sim$110 μm in diameter that were spotted with a pitch of 250 μm. Eight pins were used, each loaded with 50 nL of Ab solution. 100 spots could be printed with one loading with a contact time of 0.01 s. Sixteen identical arrays containing six replicate spots of each selected antibody were printed on each slide. Printed slides were incubated overnight at 4 °C. The layout is depicted in supplementary Fig. S2.

Washing Protocol—Slides were washed twice at room temperature with PBST for 5 min on a rotary shaker at 450 rpm followed by PBS for 5 min at 450 rpm.

ACM Protocol—The concentration of antigens and dAbs used are listed in supplementary Table S1. Sixteen-well gaskets (Proplate ®, Grace Bio-labs, Bend, OR) were clamped onto slides. All incubation steps were performed at room temperature in the dark on a shaker at 325 rpm. The slides with cAb microarrays were washed and subsequently blocked for 1 h with blocking buffer on a shaker (120 rpm). The wells were manually emptied by knocking the slides on absorbent paper. Dilution buffer spiked with antigens in a fourfold dilutions series, or diluted serum samples from breast cancer patients and normal controls, were prepared and wells were loaded with 75 μl and incubated for 1 h on a shaker (120 rpm) (supplementary Table S1). GFP was spiked at a concentration of 5 ng/ml for use as internal calibrant for signal normalization to GFP spots. The serum samples from the breast cancer patients and healthy controls were diluted four and 16 times in dilution buffer. After the antigen incubation and a washing step, the gaskets were removed and the slides were rinsed with double distilled water, blow-dry with nitrogen, and finally returned to the slide tray for dAb spotting. dAbs were diluted (supplementary Table S1) in dAb spotting buffer and were printed on top of the corresponding cAb at 75% relative humidity (see supplementary Fig. S2). Various concentrations of dAbs were tested, and 10 μg/ml found to be adequate for most pairs, but for example 50 μg/ml were used for CA15–3. This concentration is about 10 times higher than in a conventional MSA, but the volume is five orders of magnitude smaller so overall much less material is required for ACM. Once printed, the slides were left on the tray and incubated for 1 h at 75% humidity. After washing twice with PBST and once with PBS, the Proplate® gaskets were replaced and each well was loaded with 75 μl of 5 μg/ml Cy5-conjugated streptavidin (Rockland Immunochemicals) in dilution buffer and incubated for 20 min (120 rpm at room temperature). After washing, the slides were rinsed with double distilled water, blown dry under a stream of nitrogen, and stored in the dark prior to imaging with a microarray laser scanner (LS Reloaded, Tecan, Mannedorf, Switzerland).

Analysis of Cross-reactivity in 14-Plex and 8-Plex Assays—The cAbs were arrayed and the slide incubated with spiked samples as described for ACMs above, but with either a single analyte or a mixture of analytes depending on the experiment. A concentration of 32 ng/ml was used for all analytes except IL-6 and IL-8, both at 2 ng/ml reflecting the low physiological concentration of these two proteins. A single dAb or a mixture of dAbs at an individual concentration of 1 μg/ml was incubated for 1 h, followed by Cy5-conjugated streptavidin according to the ACM protocol. All washing steps were performed identically to the ACM protocol described above.

For 14-plex assays, the (cross-reactivity) signal for each cAb spot for each experiment (Fig. 3) was normalized by first subtracting the signal obtained from a negative control experiment using an array incubated with Cy5-conjugated streptavidin only. For the experiments without analyte (Fig. 3*A*) and a mixture of analytes and a single dAb (Fig. 3*B*), the signal for each cAb spot was normalized by dividing it by the signal obtained for the cAb spots with the matched dAb in Fig. 3*B*. For Fig. 3*C* the signal for each cAb spot was normalized by dividing it by the signal obtained for the cAb spots incubated with the matched analyte in Fig. 3*C*. The normalized data are shown in supplementary Table S2 (online).

Comparison of ACM with ELISA—The leptin (LEP) concentration in 20 samples from healthy donors was measured by ACM and ELISA. The ELISA kit was purchased from R&D systems, and experiment performed according to manufacturer's instructions. The samples were diluted 32 times for the ACM and 50 times for the ELISA.

Comparison of ACM and Conventional MSA—Binding curves were established for a 4-plex (LEP, HER2, GM-CSF, uPA) and a 5-plex assay (further including EGFR) using a classical antibody microarray in both MSA and ACM formats. Pooled serum from healthy donors (Innovative Research) was spiked with four proteins including LEP (150 ng/ml), HER2 (250 ng/ml), GM-CSF (12 ng/ml), and uPA (12 ng/ml) and diluted to 1:8 before being applied to the arrays and

incubated overnight. Slides for both experiments were spotted with all five cAbs and processed according to our standard operating protocols, whereas dAbs were added as a mixture (MSA) or colocalized. For the 5-plex, EGFR dAb was added to the dAb mixture.

Protein Profiling in Serum of Cancer Patients and Controls—Serum samples were obtained from 15 breast cancer patients with estrogen receptor (ER+) histological staining harboring one or more lymph node metastases. Normal serum samples were obtained from 11 healthy age-matched women undergoing reduction mammoplasty (supplementary Table S3). All sera and associated clinical data were collected at McGill University Health Center (Montreal, Canada) between 2000 and 2008 in accordance with the protocols approved by the institutional research ethics committee (MUHC SDR-99–780 and SDR-00–966-). A medical history was obtained for each patient, including medication (notably hormonal therapy), menstrual history, menopausal status, alcohol consumption. and smoking. Patient consent was obtained on an individual basis for all patients participating in this study. Blood samples (5 ml) were collected from the consenting patients in the operating room, prior to induction of anesthesia, using a venous blood collection tube BD Vacutainer™ (catalog number 369615) (BD, Franklin Lakes, NJ). The tube was left at room temperature for 60 min to permit coagulation, and then centrifuged (1300 × *g*) at 16 °C for 10 min. The serum was transferred to centrifuge tubes and centrifuged again (13,000 × *g*) at 16 °C for 2 min. The serum was then transferred to cryovials (Fisher Scientific, Ottawa, ON, Canada) and stored at −80 °C. Serum dilutions were performed in dilution buffer except when specified otherwise in the text. The stored serum aliquots were thawed and centrifuged (13000 × *g*) for 20 min at 4 °C before dilution to remove suspended particles.

Imaging Conditions and Fluorescent Intensity Signal Quantification—Fluorescence emission from Cy5 was detected at 692 nm. Detection gain was set to 100 for all experiments. Intensity and standard deviations were determined using the software program Array Pro Analyzer (MediaCybernetics, Bethesda, MD). The averaged local background of each spot was subtracted from the averaged intensity of each spot and then raw data was processed using a C++, graphical-based software developed in-house used for spot grouping, outlier removal, normalization, and basic statistical analysis. For some experiments, the signals obtained from the GFP spots were used as internal calibrators in order to normalize variations because of the pin used to create the microarrays, as well as washing and incubation steps. The concentrations were calculated with a nonlinear four-parameter logistic regression fitting using GraphPad Prism 5 (GraphPad Software Inc, La Jolla, CA). The LOD for each protein was calculated by averaging the curve fit zero values plus three standard deviations for six different standard curves. The range over which the four parameters best-fit curve and the line with the highest slope connecting two experimental data points differ by less than 5% was defined as the linear range.

Statistical Analysis—All protein expression values were converted to a log scale. Data points for which > 50% signal variation was observed among replicate spots were discarded. The Wilcoxon rank sum test and subsequence box-plots were produced by R/Bioconductor statistical software (http://www.bioconductor.org). Ward's clustering algorithm and the Euclidean distance metric were used for hierarchical clustering. All values below half of the calculated LOD were adjusted to ½ LOD for clustering and *t* test analysis.

RESULTS

Analysis of Vulnerability to Cross-reactivity in Multiplex Sandwich Assays—As discussed above, sandwich assays are characterized by their tolerance to some cross-reactivity among cAb and unrelated proteins because even in the event of cross-reactivity, no detectable signal is produced because the dAb does not bind to the protein. We introduce the concept of "liability pairs," which designates the combination of Ab-Ab, Ab-protein, or protein-protein in which a single cross-reactive binding or interaction among proteins will translate into a false positive signal (or background noise). Liability pairs do not exist in single-plex sandwich assays, but arise in MSAs following the application of a mixture of dAbs to the array. Each dAb will interact with all immobilized molecules on any of the spots. Thus, cross-reactive binding of any analyte to a cAb, protein-protein interactions among analytes, or direct cross-reactive binding of any dAb to any of the proteins immobilized on a spot will generate a false positive signal. The number of liability pairs for an array with N targets can be computed by combinatorial enumeration of each pair according to the scenarios illustrated in Fig. 2: (1) dAb-antigen, (2) dAb-cAb and (3) dAb-dAb, (4) cAb-antigen and (5) antigen-antigen. In conditions (1), (2), and (4) each of the N molecules can combinatorially encounter every other molecule in solution minus the target analyte or cognate Ab, corresponding to $(N - 1)$ interactions for each of the N spots, thus $N(N - 1)$ liability pairs for each of the three conditions. For conditions (3) and (5), the liability pairs are between the molecules within the same group and the number of pair-wise combinations are given by the binomial coefficient $\binom{N}{2} \equiv \frac{N!}{2!(N-2)!} = \frac{N(N-1)}{2}$. The number of liability pairs and the resulting vulnerability to cross-reactivity for MSAs scales as $4N(N - 1)$ with N being the number of targets in a MSA (Fig. 2*C*). The relationship between vulnerability as expressed by the scaling law, and the occurrence, and magnitude, of cross-reactive binding, false positive signals, and background noise in a MSA has not been established, and was therefore tested experimentally.

Experimental Evidence of Cross-reactivity in a 14-Plex MSA—An MSA in a microarray format with 14 targets and Abs (ANG2, EGF, EGFR, ENG, GM-CSF, FGF, uPAR, LEP, OPN, uPA, CEA, HER2, IL-6, and IL-8, see supplementary Table S1 for details) was established using commercial Ab pairs optimized for sandwich ELISAs. Cross-reactivity between reagents was assessed systematically in a series of experiments. First, (1) cross-reactivity between dAbs and cAbs was measured in a negative control experiment by incubating 14 replicate microarrays with buffer (without analytes) followed by the incubation of each array with a different dAb (Fig. 3*A*). Analyte-dependent cross-reactivity for the 14-plex array was derived by incubating 14 replicate arrays with the antigen at a concentration of 32 ng/ml in buffer according to two protocols: (2) all 14 arrays were incubated first with a mixture of all antigens followed by a single, different dAb for each (Fig. 3*B*) or (3) all 14 arrays were incubated first with a single, different antigen each, followed by a mixture of the 14 dAbs (Fig. 3*C*). The maximal cross-reactivity observed for any cAb spot in

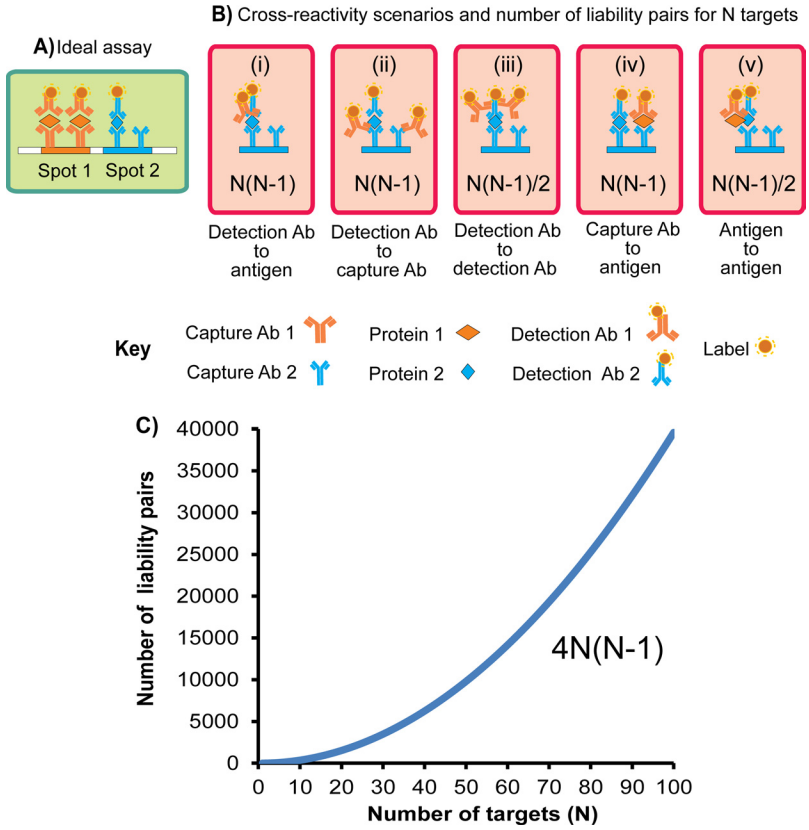

FIG. 2. **Analysis of the number of liability pairs and of the vulnerability of MSAs to cross-reactivity.** *A*, The ideal assay result (in the absence of cross-reactivity) shows protein 1 (orange) sandwiched between cAb 1 and dAb 1 on spot 1, and protein 2 (blue) sandwiched between cAb 2 and dAb 2 on spot 2; protein 1 is abundant and saturates the spots, whereas protein 2 is scarce. *B*, Five scenarios of cross-reactivity (i-v) on spot 2 occurring as a result of the cross-reaction among a pair of non-matched Abs and analytes. A false positive signal is detected when the non-matched dAb 1 cross-reacts with protein 2 (i), cAb 2 (ii), and dAb 2 (iii). Cross-reactive binding of protein 1 to respectively cAb 2 (iv) or protein 2 (v) will result in the binding of dAb1 to spot 2 and a false positive signal. The formulas in the boxes are the number of liability interactions that occur for an array with (N) targets calculated by combinatorial analysis (see SI for explanations). *C*, The total number of liability pairs increases quadratically with the number of analytes N as 4N(N-1).

each scenario (supplementary Table S2 and Fig. 3*D*) is significant, even exceeding the signal of the analyte for CEA. Additional efforts are required to uncover the source of cross-reactivity, and were undertaken for EGFR as described in the supplemental information and supplementary Fig. S3 to illustrate the challenges and efforts needed when attempting to pin down the source of interactions.

Antibody Colocalization Microarray—In an ACM, the dAbs are not applied as a mixture, but instead are each spotted at exactly the same location as the cAb on the microarray (*i.e.* colocalized) to allow for binding while eliminating all liability pairs between nonmatched Ab pairs and unrelated targets. To achieve precise overlay, registered spotting is required, which is challenging because after cAb spotting the slides are removed from the microarrayer for sample incubation and washing, and then manually placed back for spotting of the dAb (second round). Multispotting was first proposed by Angenendt *et al.* (30), and although alignment artifacts were acknowledged, it could be used for quantitative immunoassays in various formats, however its use for sandwich immunoassays was not reported. To address the alignment issue, we designed and commissioned a custom arrayer with (1) a custom-made spotting deck, (2) spring-loaded clamps to mechanically immobilize the microscope slides (supplementary Fig. S1), and (3) a pin head with a, microfabricated silicon collimator for precise alignment of the pins. The high viscosity of spotting solutions prevented the use of an inkjet, but the system included user-friendly software with flexible, graphical programming common to inkjet spotters. A customized spotting protocol for the ACM was established and an overall alignment accuracy within 20 μm achieved (supplementary Fig. S4).

Only ~1 nL of Ab is spotted and whereas this is common and unproblematic for cAbs, for dAbs the rapid evaporation of the solution interfered with the assay. Evaporation was therefore prevented by adjusting the local humidity to ~75% and adding 30% glycerol to the spotting buffers. Nitrocellulose slides were used because they suppressed nonspecific binding of the dAb observed on epoxy slides following mechanical contact between the pin and the substrate and gave a higher sensitivity. Commercial antibody pairs qualified for use in ELISAs were sourced, and tested on the ACM. Around 75% of these were found to be serviceable, allowing us to establish an ACM chip against 50 analytes (see supplementary Table S4 online).

Binding Curves and Protein Profiling with an ACM—Sixteen replicate arrays were spotted on a single slide (Figs. 4*A* and 4*B* and supplementary Fig. S2). Standard curves were established for each antibody pair using seven dilutions of each analyte in PBS and a negative control that were carried out simultaneously for all targets in eight wells (see Fig. 4*A*). Binding curves were established with a starting concentration between 2 ng/ml and 100 ng/ml (2 μg/ml for CRP) depending on the affinity so as to reach the lower LOD for each target, with 11.2 pg/ml (for CCL4) being the lowest concentration used (see Fig. 4 and supplementary Table S4).

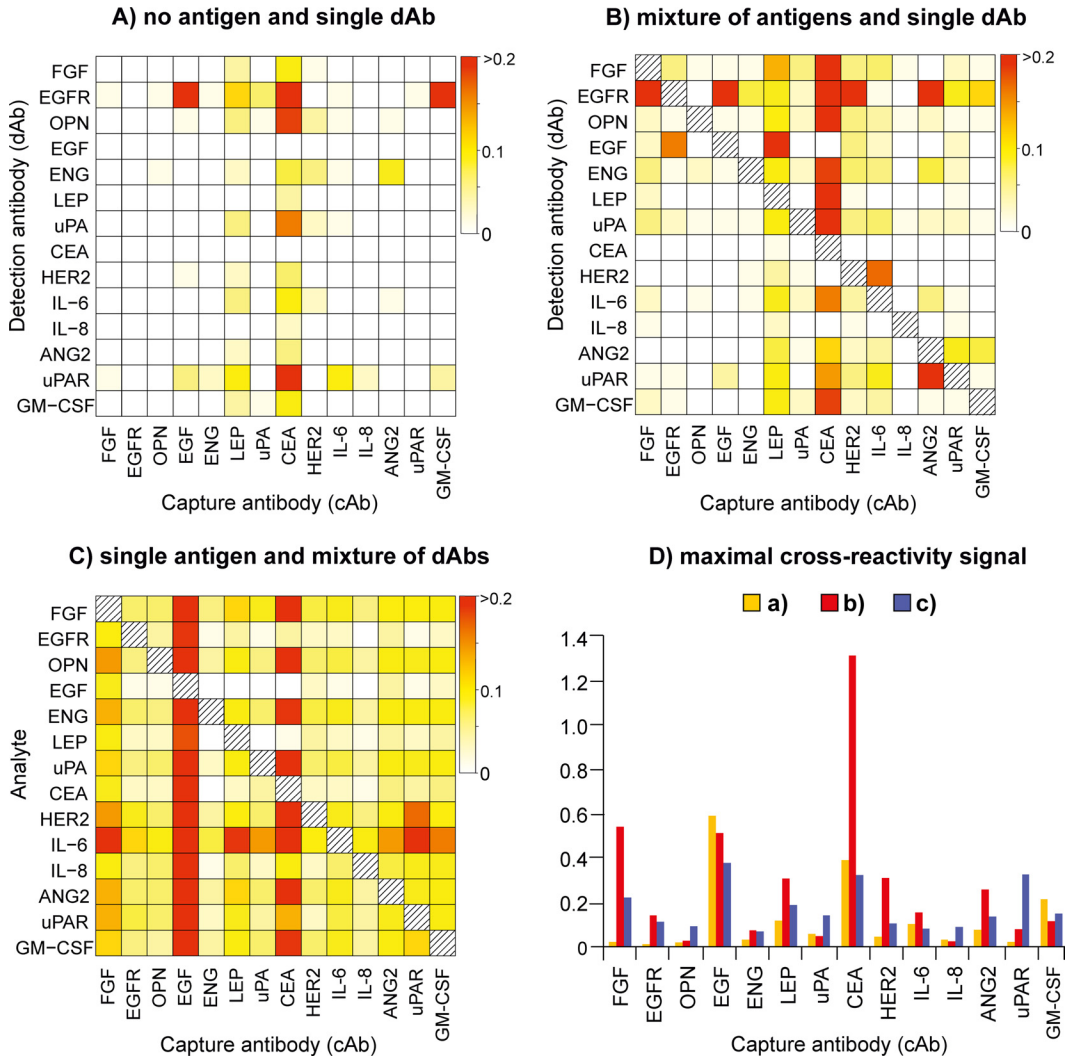

FIG. 3. **Normalized cross-reactivity maps for a MSA with 14 Ab pairs.** *A*, Fluorescence signals obtained in a negative control experiment without application of analyte followed by 14 experiments with a single dAb applied to a microarray. EGFR and uPAR dAb (rows) and CEA and LEP cAb (columns) all show significant cross-reactivity. CEA and LEP are the two Ab pairs with the weakest binding signal to their analyte at the concentration of 32 ng/ml used here making these assays vulnerable to cross-reactivity. *B*, Binding signals obtained by incubation of all arrays with a mixture of analytes followed by a single dAb each. Four columns for LEP, CEA HER2 and IL-6 are apparent, as well as rows for EGFR and to a lesser extend for uPA, suggesting that the respective cAb and the dAb are the source of cross-reactivity. For other events, it is difficult to ascribe the source. *C*, Signals observed upon incubating each array with a single antigen followed by a mixture of dAbs. Cross-reactivity signals are widespread indicating that mixing of dAbs is the primary source of cross-reactivity. *D*, Comparison of the maximal cross-reactivity signal for each cAb in (*A-C*) for the three different experiments. On aggregate, the cross-reactivity signal adds up to more than 50% of the binding signal for three analytes, >20% for eight, >10% for eleven, and >5% for all fourteen. These results indicate that cross-reactivity originates from multiple sources and will affect the accuracy for each target in this 14-plex MSA.

To assess the potential of the ACM for profiling of proteins in blood, we sought the physiological concentration of proteins used on the array and compared them to the LOD of each assay (see supplementary Table S5). Results indicate that the performance of the ACM is adequate to detect many proteins at their physiological concentration in four times diluted serum used here, with the exception of some cytokines that are found in the low pg/ml range. However, because the protein concentration may increase in diseases such as cancer, it is reasonable to include these in the array.

Comparison of ACM with ELISA and MSA—To verify that the results obtained with ACM are comparable to ELISA, the concentration of leptin (LEP) in 20 serum samples of healthy persons was measured using both methods (Fig. 5*A*) and the results found to be highly correlated (R^2 = 0.95). Next, the ACM and a conventional MSA antibody microarrays were performed side by side. Pooled serum of healthy patients was profiled with a 4-plex assay against HER2, LEP, GM-CSF, uPA (which were all spiked in as they were undetectable otherwise) and a 5-plex (including EGFR, which was not

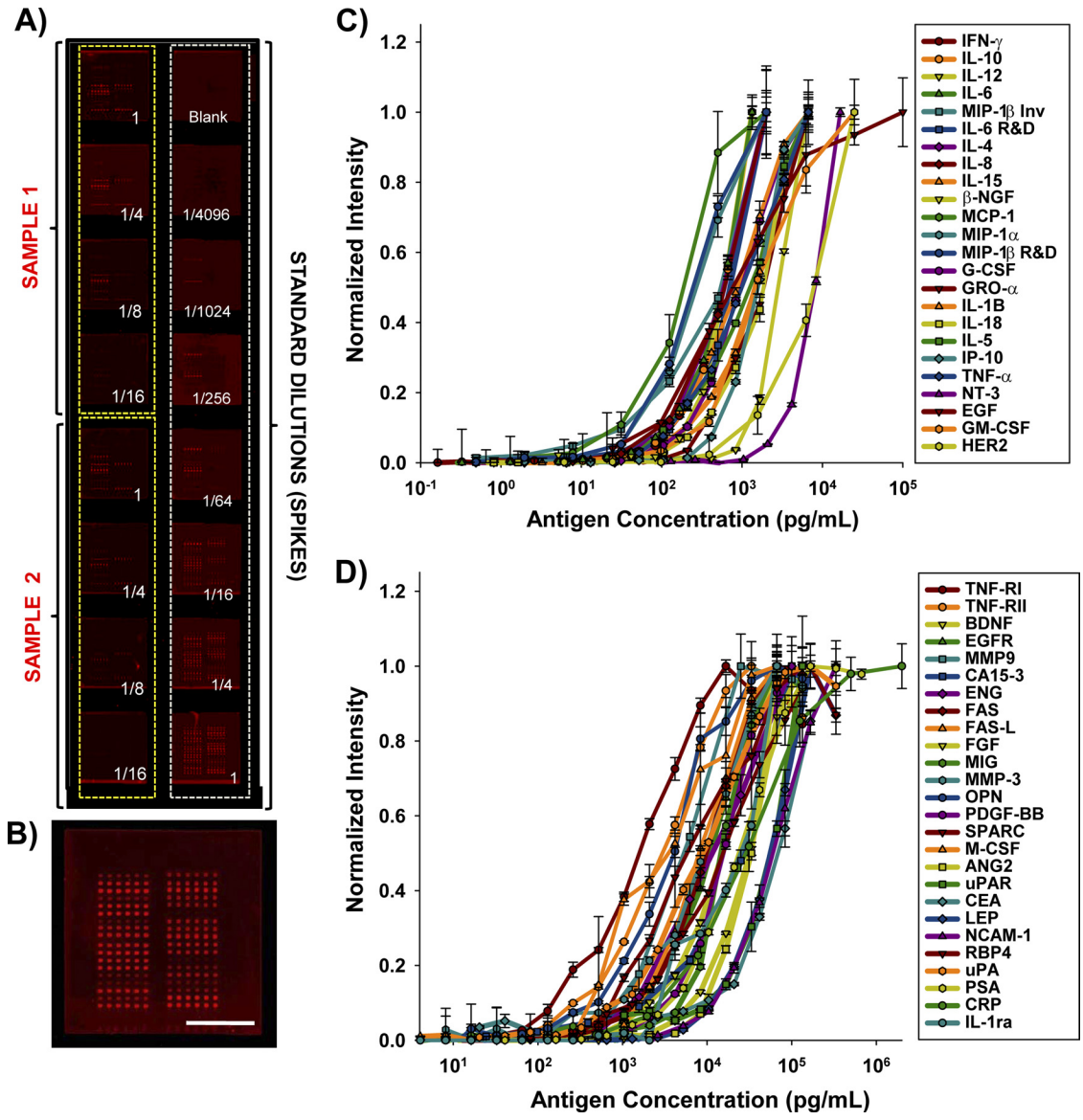

FIG. 4. **ACM layout and binding curves for 50 Ab pairs including all 14 proteins and Abs analyzed as part of a MSA shown in Fig. 3.** *A*, Fluorescent micrograph of a representative slide with 16 replicate arrays incubated with two serum samples and corresponding dilutions (*left*), and buffer solution with recombinant proteins with seven dilutions and a negative control used to establish the standard curves (*right*). *B*, Detail of a single array with six replicate spots for each analyte forming a line. Standard binding curves of Ab pairs with lower (*C*) and higher (*D*) sensitivity that extend into the low pg/ml range (for CRP the concentration is in ng/ml). Lines are guide to the eye. Scale bar in (*B*): 2 mm.

spiked in). EGFR was left-out in one experiment and added in the other experiment because it had been found that the dAb cross-reacted with GM-CSF (Fig. 3*A*), and with other proteins (Figs. 3*B* and 3*C*), and so we wanted to test whether this would be reflected in a serum sample. A statistically significant increase in the signal for GM-CSF for MSAs (20%) (Fig. 5*B*), but not for the ACM, was observed after the addition of EGFR dAb. It is interesting to note the high signal of the EGFR spot in the absence of EGFR dAb, which reflects high cross-reactivity of other dAbs against the EGFR protein or the cAb, or both. The other cross-reactivity events between EGFR and the other targets did not meet the condition of statistical significance in this experiment. For targets found at higher concentrations, one would expect cross reactivity to be less problematic because the intrinsic high signal of the target, which applies to this experiment because the four target proteins were spiked in. Furthermore, Fig. 3 reports the cross-reactivity from 14 reagents, whereas only five were used here. Moreover, EGFR antigen was also present in the 4-plex, and thus the cross-reactivity of other four dAbs to the EGFR protein would be occurring in both MSAs and could not be detected in this experiment. In conclusion, the interaction in Fig. 3*A* was the only one that would occur with certainty in this experiment, and it was identified.

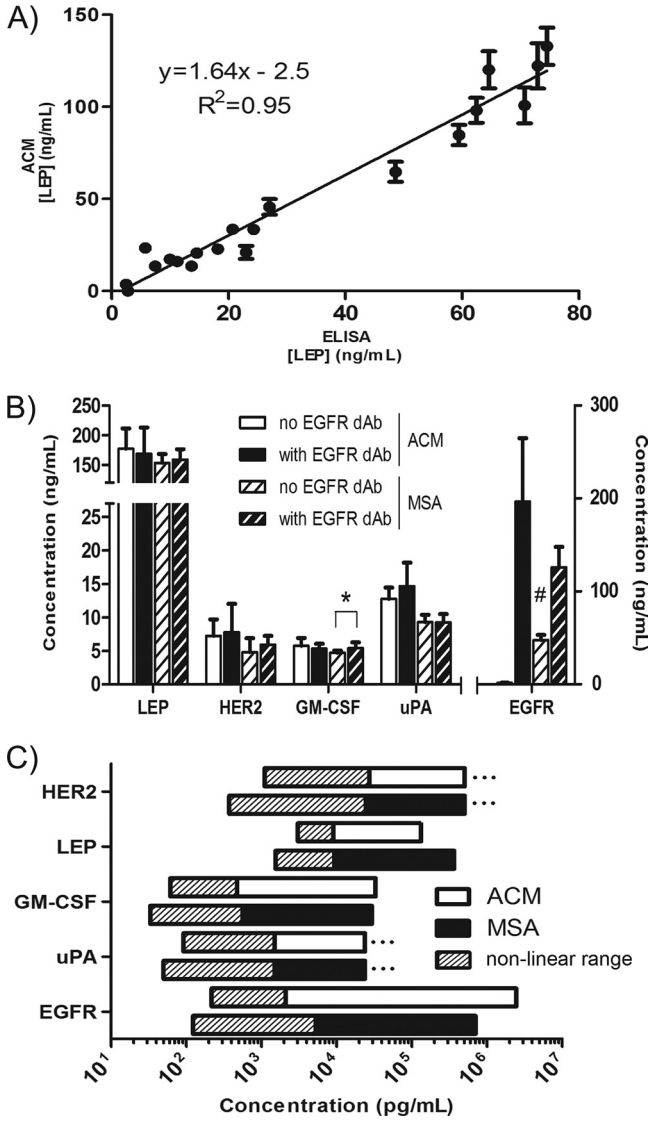

FIG. 5. **Comparison of ACM with ELISA and MSA.** *A*, Graphic showing the **c**oncentration of LEP measured in 20 serum samples from healthy donors with an ACM and a commercial ELISA kit. Error bars denote the variation of six replicate spots of the ACM. An excellent correlation ($R^2 = 0.95$) is obtained between the two methods. *B*, Concentration of HER2, LEP, GMCSF, uPA, and EGFR measured using a 4-plex and a 5-plex (without and with EGFR dAb, respectively) antibody microarray in both MSA format and ACM format. The results obtained with ACM and MSA are similar. The addition of EGFR dAb to the assay leads to a significant increase (* $p < 0.05$) for the concentration of GM-CSF for the MSA assay, consistent with the cross-reactivity map reported in Fig. 3*A*; no significant changes were measured for the ACM. Please note (#) the high signal for EGFR in the 4-plex MSA without EGFR dAb that is indicative of cross-reaction toward the EGFR protein and/or cAb, and which presumably skews the result obtained in the 5-plex assay with EGFR dAb. *C*, The linear range of ACM (open bars) and MSA (closed bars) assays and LODs (left most point of hatched bar). Three dots indicate that the last experimental data point was within the linear range. Both assay formats are consistent and their linear range is between one to four orders of magnitude depending on the analyte.

Characteristics of the binding curves for the MSA and ACM for the 4- and 5-plex assays are reported in Fig. 5*C*. The LODs and linear range of both assay formats are consistent, further validating the ACM. The linear range for EGFR is longer in the ACM format, which may be attributed to the cross-reaction in the MSA format (Fig. 5*B*). The lower LODs for MSA are approximately a factor two lower than for the ACM in these experiments in this 5-plex format. The second spotting round introduces additional variability which directly affects the lower LOD, and for low multiplexing values, MSAs are thus more precise, However, these experiments show that whereas the precision—describing the reproducibility of independent measurements—may be good and the LODs low, the accuracy—describing how close the measurements are to the real value—may in fact be compromised because cross-reactivity can skew all values while remaining hidden to the experimenter, as illustrated by EGFR (Fig. 5*B*). ACM are still being optimized and the LODs will approach the one for MSAs, and exceed it for large scale multiplexing.

Multiplexed Protein Profiling in Complex Samples—Blood is widely recognized as one of the most challenging samples for proteomics analysis (13) and was used to validate the ACM by profiling 32 proteins in the serum of (i) 15 patients with primary breast cancer overexpressing the estrogen receptor (ER) in the primary tumor (ER+ subtype), and of (ii) 11 controls from age-matched patients undergoing reduction mammoplasties (see supplementary Tables S3 and S6). The samples were collected prior to surgery and therapeutic intervention. Six proteins (ENG, LEP, OPN, IL-1B, TNF-α, and uPAR) were correlated with the cancer status of the patient as shown in Figs. 6*A*–6*F*. Receiver-operator characteristic (ROC) curves along with the area under the curve (AUC) for the three best candidate biomarkers are shown in Figs. 6*G*–6*I*. These results illustrate the ability of the ACM to distinguish between healthy and breast disease using protein levels in patient sera. Hierarchical clustering (a simple form of multivariate analysis) of these six proteins across all patients is also able to discriminate between cancer and noncancer samples (Fig. 6*J*).

DISCUSSION

Five scenarios of pair-wise cross-reactivity (Fig. 2*B*) can arise because of the mixture of dAbs used when probing a microarray in a sandwich assay format. The first scenario (i) is the binding of a dAb to a nontarget antigen immobilized to the surface. Because of the overall excess of dAbs relative to bound analytes, even low-affinity cross-reactivity may produce or increase the fluorescent signal detected by binding a different epitope. The second scenario (ii) is cross-reactivity between dAbs and cAbs or impurities on the spot. The third scenario (iii) is cross-reactivity among the dAbs. The fourth scenario (iv) is cross-reactivity between antigen and cAbs. This occurrence is most problematic when working with blood samples because the dynamic range of protein concentration covers at least 10 orders of magnitude. Thus, for example, a

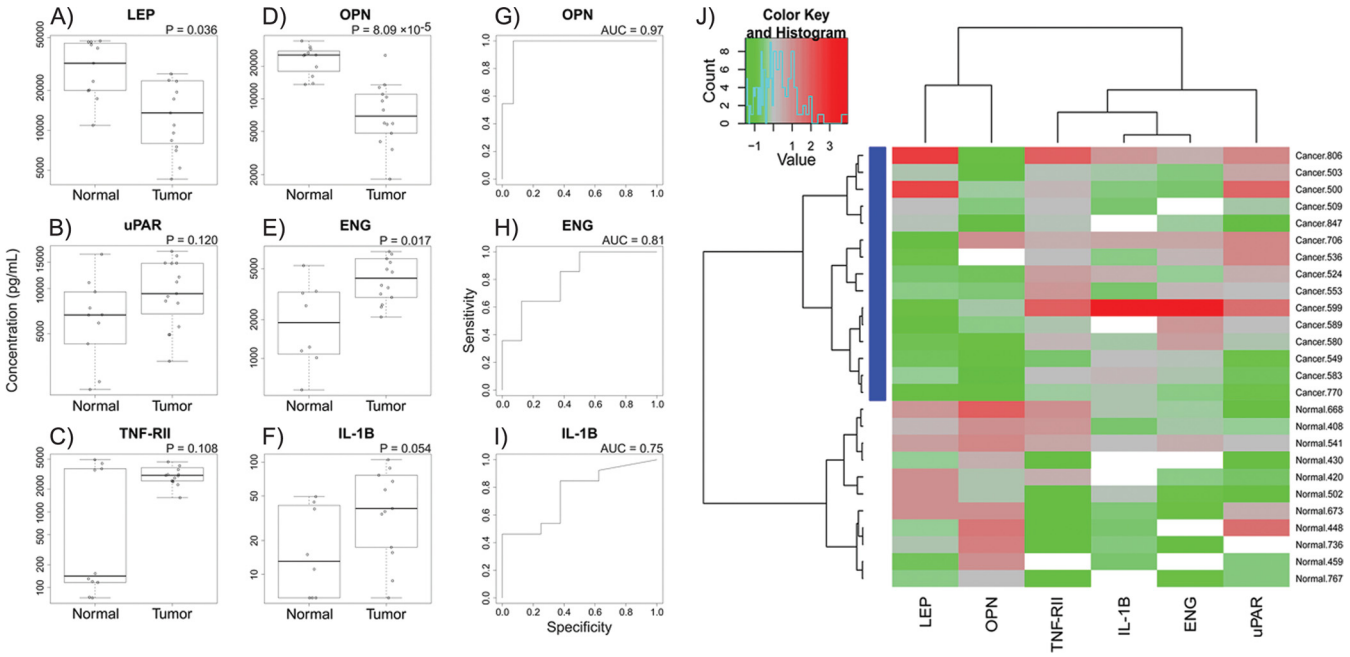

FIG. 6. **Proteins differentially expressed in the serum of breast cancer patients and of healthy controls.** (*A–F*) Logarithmic box plots of the concentration in pg/ml of six proteins in 11 controls (*left* box plot) and 15 breast cancer patients (*right* box plot). The boxes indicate the upper and lower quartile; the line is the median value and the whiskers show the range. The *p* value according to the Wilcoxon rank sum test is shown above the plot. OPN has the strongest discriminatory power with a *p* value of 8.09×10^{-5}. (*G–I*) ROC curves corresponding to graphs (*D–F*), yielding AUC values of 0.97 for OPN, 0.81 for ENG and. 0.75 for IL-1B. (*J*) Hierarchical cluster analysis based on the six proteins. To allow comparison between different analytes with each different average concentrations and range, the concentration was converted to a log scale and mean transformed. The resulting color coding and Z scores are shown in the *top left* corner. White squares constitute data that were variable and were not used for clustering calculation. Estrogen receptor positive (ER+) breast cancer patients (highlighted in blue on the left) clustered at the top and healthy controls at the bottom. These results suggest that these six proteins might serve as biomarkers for diagnosis or prognosis of breast cancer.

cAb with low micromolar affinity toward a non-related protein that is at μg/ml concentration in the sample will give rise to a false positive signal that may mask the target protein if it is present at pg/ml only. Finally the fifth scenario (v) arises from the cross-reactivity because of the formation of antigen complexes that leads to the overestimation of signal corresponding to the incorrect antigen. Protein interactions and complexes were widely studied using MS (31–35), yet were usually not considered in the context of protein profiling on Ab microarrays. The Haab group however recently established a microarray-based protocol to study them (36), thus proving their existence and confirming that they could skew the signal. Please note that scenario (iv) also occurs in single-step assays that rely on direct sample labeling or that use label-free biosensors, but with the difference that any protein in the sample could contribute to a false positive whereas in MSAs only proteins targeted on the array constitute a liability thanks to the discrimination afforded by the dAbs.

The sum of liability pairs in relation to the array of size N corresponding to the enumeration of all the combinations (1–5) shown in Fig. 2*C* follows the quadratic scaling law $4N(N-1)$. This number represents a quantitative measure of the vulnerability to cross-reactivity of MSAs due to liability pairs. Pair-wise interactions of cAb-cAb were not considered because they do not occur on a microarray but they may need to be considered for bead assays where they may occur (although depending on bead size it may be negligible), and the scaling law under this scenario becomes $9N(N-1)/2$.

The multiple cross-reactivity signals observed and the impact from a single low quality reagent, such as the CEA cAb or the EGFR dAb (see Fig. 3) illustrate the consequences of this vulnerability. These findings were corroborated by the 4- and 5-plex assays performed with pooled serum with both ACM and MSA with and without EGFR dAbs. Whereas in our hands 5-plex MSAs had low standard deviations (Fig. 5), MSAs have been found to suffer from high variability for bead-based assays with moderate multiplexing of 10–20 analytes (37–40). Vulnerability and the quadratic increase of liability pairs can help explain these results.

The quadratic scaling law and widespread cross-reactivity identified in a 14-plex assay can account for the difficulty in scaling up MSAs beyond a few tens of targets. Testing and optimization help reduce cross-reactivity by selecting suitable Abs, yet alternative Abs are difficult to find and sometimes not available, and the conditions of the test may not reflect the ones encountered in practice. Indeed, different samples and sample matrices will likely result in untested assay conditions that may give rise to cross-reactivity. In addition, for large

MSAs, additional false positive signals may arise following dual cross-reaction of a sample protein with a nonmatched cAb and dAb. Finally, based on the results in Figs. 5*B* and 5*C*, an MSA may show low standard deviation and excellent LODs, but because cross-reactivity may skew the results, in practice have a poor accuracy and a reduced linear range.

In ACM, the matched cAb and dAb are the only "liability pair" for each target which explains why the ACM is not susceptible to cross-reactivity. Indeed, each assay on the array is confined to a single spot and supplied with 1 nL of dAb, constituting a nano-sandwich assay (or "nano-ELISAs", see Fig. 1). Only the interferences that affect sandwich assays (20) need to be considered for ACM, and for each target it is independent of the total number of targets. Whereas each Ab must pass the test of cross-reactivity to all other reagents for use in MSAs, for an ACM only affinity and LOD need to be considered, as in single-plex ELISA. The 14 Ab pairs found to broadly cross-react in a MSA (Fig. 3) were all serviceable for the 50-plex ACM (Fig. 4). ACMs require a more complex infrastructure for precise alignment and are more labor intensive as they necessitate a second round of spotting to be performed following sample incubation. These efforts are rewarded by minimizing liability and the risk of cross-reactivity. An MSA or a multiplicity of MSAs with limited multiplexing may be used for applications where the concentration of the analytes is high, the number of targets per MSA assay low, and the risk of cross-reactivity small. For applications where either the analytes are at low concentration, or the number of targets large, or the sample is scarce, or where skewed results and false positives can have important consequences (such as for clinical diagnosis), the use of ACM will be recommended.

Identifying and validating cancer biomarkers in blood is one of the most challenging application for proteomics owing to the low concentration of many biomarkers and the high concentration of many blood proteins. For breast cancer, only a few studies have been published, notably by the Borrebaeck group who used an antibody microarray and direct labeling in two studies. The first aimed at comparing the concentration of proteins in the blood of metastatic patients receiving therapy (with presumably a heavy tumor load) (9) compared with controls. The second study measured proteins in the serum collected before and several months after breast cancer surgery, and established a prognostic biomarker panel based on the difference in concentration (14). Another study used MSA on beads against 35 targets and found candidate biomarkers in the serum of nonmetastatic patients, however 12 assays were performed separately owing to cross-reactivity among reagents (25). In our study, the serum sample was collected shortly after the diagnosis of cancer from patients that were not metastatic and had not received adjuvant therapy. The candidate biomarkers that we identified (Fig. 6) agree with the results of prior studies which reported increased concentrations of uPAR (41), TNF-RII (42), IL-1B (25), and ENG (43) and are consistent with known breast cancer biology. OPN and LEP were decreased in the ER+ patients in our study. LEP concentration in blood of cancer patients is usually increased (44), but was found to be decreased in at least one study (45). Leptin concentration is highly correlated with fat storage and body mass index (46) and, breast hypertrophy correlates with body mass index (47), hence, it is plausible that our control group (breast reduction mammoplasty patients) would have increased LEP concentrations in serum. OPN was previously found to be overexpressed in breast cancer (48), but it was shown to be negatively correlated to ER+ and luminal subtype (49) while it is also known to be expressed in healthy breast stroma (6), which is hypertrophic in our control group. The candidate biomarkers identified here may be valuable for early diagnosis or for subtype assignment, but will need to be confirmed in follow-up studies with larger number of patients and controls. These results show that ACM may be used for profiling multiple proteins in complex samples, notably for biomarker studies.

In this study, we have elucidated how mixing of reagents—which was considered inherent to MSA—creates liability pairs that scale as $4N(N-1)$ and increase vulnerability to cross-reactivity. These results, together with widespread cross-reactivity observed in a 14-plex MSA, substantiate that the high sensitivity and specificity associated with sandwich assays is compromised upon multiplexing, and that scaling of MSAs with current methods is unfeasible. Vulnerability and robustness are powerful concepts to characterize complex systems and networks (50), and our results suggest that assays, and by extension biosensors and diagnostics, may also benefit from such analysis to identify and quantify vulnerabilities, and overcome them. Based on our analysis, we introduced the ACM with nano-sandwich assays which avoids mixing of dAbs. ACMs with up to 50 Ab pairs were established while including many pairs that cross-reacted in an MSA, and compared with ELISA and MSAs. Abs were spotted with a 250 μm center-to-center spacing in each of the sixteen 6×6 mm^2 wells that could readily accommodate up to 529 spots. Scaling up the array to include all ~21,400 protein-coding genes in humans could be achieved using a 40-μm-spacing between spots, or by using a full slide for one array. The main challenge to scaling up the ACM in the short term is the availability and quality cAb-dAb pairs and antigens (51), and their cost ($500–1500 per set). The choice of ACM for biomarker validation over MS will clearly depend on the availability of binders against larger faction of the human proteome (52). Conversely, the ACM format and the elimination of combinatorial liability pairs will help accelerate the scaling up of antibody chips for protein analysis. The throughput of ACM-chip based tests could be high, and the cost relatively low, if produced on a large scale. The sensitivity of the ACM will be improved with additional efforts, for instance by integrating nanowells (53) and microfluidics (27, 54), and by combining it with single molecule assays (19, 55) with fg/ml sensitivity. ACMs have the potential to become a powerful tool for biomarker discovery and validation.

Acknowledgments—We thank J. M. Bergeron for helpful discussions and support and R. Sladek for proof reading. M.P.-R. acknowledges financial support from Spanish Ministry of Science trough a post-doctoral fellowship. D. J. holds a Canada Research Chair and M. P. holds the Diane and Sal Guerrera Chair in Cancer Genetics at McGill University.

* This work was supported by the Canadian Institutes for Health Research (CIHR), Genome Canada, Genome Quebec the Canada Foundation for Innovation (CFI), The Natural Science and Engineering Research Council (NSERC), the Banque de tissue et de données of the Réseau de la Recherches sur le cancer (RRCancer) of the Fonds de Recherche en Santé du Québec (FRSQ).

S This article contains supplemental Figs. S1 to S4 and Tables S1 to S6.

|||| To whom correspondence should be addressed: Biomedical Engineering Department, McGill University and Genome Quebec Innovation Centre, Department of Neurology and Neurosurgery, McGill University, 740 Dr. Penfield Avenue, H3A 1A4, Montreal, Quebec, Canada. Tel.: + 1 (514) 398 7676; Fax: + 1 (514) 398 1790; E-mail: david.juncker@mcgill.ca.

REFERENCES

1. Moore, G. E. (2003) No exponential is forever: but "Forever" can be delayed! *Proceedings of the IEEE Solid-State Circuits Conference (ISSCC)*, pp. 20–23 vol. 21
2. Pease, A. C., Solas, D., Sullivan, E. J., Cronin, M. T., Holmes, C. P., and Fodor, S. P. (1994) Light-generated oligonucleotide arrays for rapid DNA sequence analysis. *Proc. Natl. Acad. Sci. U. S. A.* **91,** 5022–5026
3. Ragoussis, J., and Elvidge, G. (2006) Affymetrix GeneChip® system: moving from research to the clinic. *Exp. Rev. Mol. Diagnostics* **6,** 145–152
4. Eisen, M. B., Spellman, P. T., Brown, P. O., and Botstein, D. (1998) Cluster analysis and display of genome-wide expression patterns. *Proc. Natl. Acad. Sci. U. S. A.* **95,** 14863–14868
5. van de Vijver, M. J., He, Y. D., van't Veer, L. J., Dai, H., Hart, A. A., Voskuil, D. W., Schreiber, G. J., Peterse, J. L., Roberts, C., Marton, M. J., Parrish, M., Atsma, D., Witteveen, A., Glas, A., Delahaye, L., van der Velde, T., Bartelink, H., Rodenhuis, S., Rutgers, E. T., Friend, S. H., and Bernards, R. (2002) A gene-expression signature as a predictor of survival in breast cancer. *N. Engl. J. Med.* **347,** 1999–2009
6. Finak, G., Bertos, N., Pepin, F., Sadekova, S., Souleimanova, M., Zhao, H., Chen, H., Omeroglu, G., Meterissian, S., Omeroglu, A., Hallett, M., and Park, M. (2008) Stromal gene expression predicts clinical outcome in breast cancer. *Nat. Med.* **14,** 518–527
7. Hoheisel, J. D., and Vingron, M. (2000) Transcriptional profiling: is it worth the money? *Res. Microbiol.* **151,** 113–119
8. Ekins, R., Chu, F., and Biggart, E. (1989) Development of microspot multianalyte ratiometric immunoassay using dual fluorescent-labelled antibodies. *Anal. Chim. Acta* **227,** 73–96
9. Carlsson, A., Wingren, C., Ingvarsson, J., Ellmark, P., Baldertorp, B., Fernö, M., Olsson, H., and Borrebaeck, C. A. (2008) Serum proteome profiling of metastatic breast cancer using recombinant antibody microarrays. *Eur. J. Cancer* **44,** 472–480
10. Schwenk, J. M., Gry, M., Rimini, R., Uhlén, M., and Nilsson, P. (2008) Antibody Suspension Bead Arrays within Serum Proteomics. *J. Proteome Res.* **7,** 3168–3179
11. Qavi, A. J., Washburn, A. L., Byeon, J. Y., and Bailey, R. C. (2009) Label-free technologies for quantitative multiparameter biological analysis. *Anal. Bioanal. Chem.* **394,** 121–135
12. Lutz, A. M., Willmann, J. K., Cochran, F. V., Ray, P., and Gambhir, S. S. (2008) Cancer screening: a mathematical model relating secreted blood biomarker levels to tumor sizes. *PLoS Med.* **5,** e170
13. Anderson, N. L., and Anderson, N. G. (2002) The Human Plasma Proteome: History, Character, and Diagnostic Prospects. *Mol. Cell. Proteomics* **1,** 845–867
14. Carlsson, A., Wingren, C., Kristensson, M., Rose, C., Fernö, M., Olsson, H., Jernström, H., Ek, S., Gustavsson, E., Ingvar, C., Ohlsson, M., Peterson, C., and Borrebaeck, C. A. K. (2011) Molecular serum portraits in patients with primary breast cancer predict the development of distant metastases. *Proc. Natl. Acad. Sci. U. S. A.* **108,** 14252–14257
15. Holm, A., Wu, W., and Lund-Johansen, F. Antibody array analysis of labelled proteomes: how should we control specificity? *New Biotechnol.*, in press
16. Addona, T. A., Abbatiello, S. E., Schilling, B., Skates, S. J., Mani, D. R., Bunk, D. M., Spiegelman, C. H., Zimmerman, L. J., Ham, A. J., Keshishian, H., Hall, S. C., Allen, S., Blackman, R. K., Borchers, C. H., Buck, C., Cardasis, H. L., Cusack, M. P., Dodder, N. G., Gibson, B. W., Held, J. M., Hiltke, T., Jackson, A., Johansen, E. B., Kinsinger, C. R., Li, J., Mesri, M., Neubert, T. A., Niles, R. K., Pulsipher, T. C., Ransohoff, D., Rodriguez, H., Rudnick, P. A., Smith, D., Tabb, D. L., Tegeler, T. J., Variyath, A. M., Vega-Montoto, L. J., Wahlander, A., Waldemarson, S., Wang, M., Whiteaker, J. R., Zhao, L., Anderson, N. L., Fisher, S. J., Liebler, D. C., Paulovich, A. G., Regnier, F. E., Tempst, P., and Carr, S. A. (2009) Multi-site assessment of the precision and reproducibility of multiple reaction monitoring-based measurements of proteins in plasma. *Nat. Biotechnol.* **27,** 633–641
17. Addona, T. A., Shi, X., Keshishian, H., Mani, D. R., Burgess, M., Gillette, M. A., Clauser, K. R., Shen, D., Lewis, G. D., Farrell, L. A., Fifer, M. A., Sabatine, M. S., Gerszten, R. E., and Carr, S. A. (2011) A pipeline that integrates the discovery and verification of plasma protein biomarkers reveals candidate markers for cardiovascular disease. *Nat. Biotechnol.* **29,** 635–643
18. Whiteaker, J. R., Lin, C., Kennedy, J., Hou, L., Trute, M., Sokal, I., Yan, P., Schoenherr, R. M., Zhao, L., Voytovich, U. J., Kelly-Spratt, K. S., Krasnoselsky, A., Gafken, P. R., Hogan, J. M., Jones, L. A., Wang, P., Amon, L., Chodosh, L. A., Nelson, P. S., McIntosh, M. W., Kemp, C. J., and Paulovich, A. G. (2011) A targeted proteomics-based pipeline for verification of biomarkers in plasma. *Nat. Biotechnol.* **29,** 625–634
19. Rissin, D. M., Kan, C. W., Campbell, T. G., Howes, S. C., Fournier, D. R., Song, L., Piech, T., Patel, P. P., Chang, L., Rivnak, A. J., Ferrell, E. P., Randall, J. D., Provuncher, G. K., Walt, D. R., and Duffy, D. C. (2010) Single-molecule enzyme-linked immunosorbent assay detects serum proteins at subfemtomolar concentrations. *Nat. Biotechnol.* **28,** 595–599
20. Selby, C. (1999) Interference in immunoassay. *Ann. Clin. Biochem.* **36,** 704–721
21. Kakabakos, S. E., Christopoulos, T. K., and Diamandis, E. P. (1992) Multianalyte immunoassay based on spatially distinct fluorescent areas quantified by laser-excited solid-phase time-resolved fluorometry. *Clin. Chem.* **38,** 338–342
22. Zichi, D., Eaton, B., Singer, B., and Gold, L. (2008) Proteomics and diagnostics: Let's Get Specific, again. *Curr. Opin. Chem. Biol.* **12,** 78–85
23. Perlee, L., Christiansen, J., Dondero, R., Grimwade, B., Lejnine, S., Mullenix, M., Shao, W. P., Sorette, M., Tchernev, V. T., Patel, D. D., and Kingsmore, S. F. (2004) Development and standardization of multiplexed antibody microarrays for use in quantitative proteomics. *Proteome Sci.* **2,** 1–22
24. Gonzalez, R. M., Seurynck-Servoss, S. L., Crowley, S. A., Brown, M., Omenn, G. S., Hayes, D. F., and Zangar, R. C. (2008) Development and validation of sandwich ELISA microarrays with minimal assay interference. *J. Proteome Res.* **7,** 2406–2414
25. Kim, B. K., Lee, J. W., Park, P. J., Shin, Y. S., Lee, W. Y., Lee, K. A., Ye, S., Hyun, H., Kang, K. N., Yeo, D., Kim, Y., Ohn, S. Y., Noh, D. Y., and Kim, C. W. (2009) The multiplex bead array approach to identifying serum biomarkers associated with breast cancer. *Breast Cancer Res.* **11,** R22
26. Brennan, D. J., O'Connor, D. P., Rexhepaj, E., Ponten, F., and Gallagher, W. M. (2010) Antibody-based proteomics: fast-tracking molecular diagnostics in oncology. *Nat. Rev. Cancer* **10,** 605–617
27. Fan, R., Vermesh, O., Srivastava, A., Yen, B. K. H., Qin, L., Ahmad, H., Kwong, G. A., Liu, C. C., Gould, J., Hood, L., and Heath, J. R. (2008) Integrated barcode chips for rapid, multiplexed analysis of proteins in microliter quantities of blood. *Nat. Biotechnol.* **26,** 1373–1378
28. Mitchell, P. (2010) Proteomics retrenches. *Nat. Biotechnol.* **28,** 665–670
29. Schneiderhan-Marra, N., Sauer, G., Kazmaier, C., Hsu, H. Y., Koretz, K., Deissler, H., and Joos, T. (2010) Multiplexed immunoassays for the analysis of breast cancer biopsies. *Anal. Bioanal. Chem.* **397,** 3329–3338
30. Angenendt, P., Glökler, J., Konthur, Z., Lehrach, H., and Cahill, D. J. (2003) 3D Protein Microarrays: Performing Multiplex Immunoassays on a Single Chip. *Anal. Chem.* **75,** 4368–4372
31. Gingras, A. C., Gstaiger, M., Raught, B., and Aebersold, R. (2007) Analysis of protein complexes using mass spectrometry. *Nat. Rev. Mol. Cell Biol.*

8, 645–654
32. Gavin, A.-C., Bösche, M., Krause, R., Grandi, P., Marzioch, M., Bauer, A., Schultz, J., Rick, J. M., Michon, A.-M., Cruciat, C.-M., Remor, M., Hofert, C., Schelder, M., Brajenovic, M., Ruffner, H., Merino, A., Klein, K., Hudak, M., Dickson, D., Rudi, T., Gnau, V., Bauch, A., Bastuck, S., Huhse, B., Leutwein, C., Heurtier, M.-A., Copley, R. R., Edelmann, A., Querfurth, E., Rybin, V., Drewes, G., Raida, M., Bouwmeester, T., Bork, P., Seraphin, B., Kuster, B., Neubauer, G., and Superti-Furga, G. (2002) Functional organization of the yeast proteome by systematic analysis of protein complexes. *Nature* **415,** 141–147
33. Ptacek, J., Devgan, G., Michaud, G., Zhu, H., Zhu, X., Fasolo, J., Guo, H., Jona, G., Breitkreutz, A., Sopko, R., McCartney, R. R., Schmidt, M. C., Rachidi, N., Lee, S.-J., Mah, A. S., Meng, L., Stark, M. J., Stern, D. F., De Virgilio, C., Tyers, M., Andrews, B., Gerstein, M., Schweitzer, B., Predki, P. F., and Snyder, M. (2005) Global analysis of protein phosphorylation in yeast. *Nature* **438,** 679–684
34. Stark, C., Breitkreutz, B. J., Reguly, T., Boucher, L., Breitkreutz, A., and Tyers, M. (2006) BioGRID: a general repository for interaction datasets. *Nucleic Acids Res.* **34,** D535–D539
35. Jensen, L. J., Kuhn, M., Stark, M., Chaffron, S., Creevey, C., Muller, J., Doerks, T., Julien, P., Roth, A., Simonovic, M., Bork, P., and von Mering, C. (2009) STRING 8—a global view on proteins and their functional interactions in 630 organisms. *Nucleic Acids Res.* **37,** D412–D416
36. Bergsma, D., Chen, S., Buchweitz, J., Gerszten, R., and Haab, B. B. (2010) Antibody-array interaction mapping, a new method to detect protein complexes applied to the discovery and study of serum amyloid P interactions with kininogen in human plasma. *Mol. Cell. Proteomics* **9,** 446–456
37. Fu, Q., Zhu, J., and Van Eyk, J. E. (2010) Comparison of multiplex immunoassay platforms. *Clin. Chem.* **56,** 314–318
38. Ellington, A. A., Kullo, I. J., Bailey, K. R., and Klee, G. G. (2010) Antibody-based protein multiplex platforms: technical and operational challenges. *Clin. Chem.* **56,** 186–193
39. Ellington, A. A., Kullo, I. J., Bailey, K. R., and Klee, G. G. (2009) Measurement and quality control issues in multiplex protein assays: a case study. *Clin. Chem.* **55,** 1092–1099
40. Djoba Siawaya, J. F., Roberts, T., Babb, C., Black, G., Golakai, H. J., Stanley, K., Bapela, N. B., Hoal, E., Parida, S., van Helden, P., and Walzl, G. (2008) An evaluation of commercial fluorescent bead-based luminex cytokine assays. *PLoS ONE* **3,** e2535
41. Stephens, R. W., Pedersen, A. N., Nielsen, H. J., Hamers, M. J., Hoyer-Hansen, G., Ronne, E., Dybkjaer, E., Dano, K., and Brünner, N. (1997) ELISA determination of soluble urokinase receptor in blood from healthy donors and cancer patients. *Clin. Chem.* **43,** 1868–1876
42. Aderka, D., Englemann, H., Hornik, V., Skornick, Y., Levo, Y., Wallach, D., and Kushtai, G. (1991) Increased serum levels of soluble receptors for tumor necrosis factor in cancer patients. *Cancer Res.* **51,** 5602–5607
43. Vo, M. N., Evans, M., Leitzel, K., Ali, S. M., Wilson, M., Demers, L., Evans, D. B., and Lipton, A. (2010) Elevated plasma endoglin (CD105) predicts decreased response and survival in a metastatic breast cancer trial of hormone therapy. *Breast Cancer Res. Treat.* **119,** 767–771
44. Somasundar, P., McFadden, D. W., Hileman, S. M., and Vona-Davis, L. (2004) Leptin is a growth factor in cancer. *J. Surg. Res.* **116,** 337–349
45. Pietrowska, M., Marczak, L., Polanska, J., Behrendt, K., Nowicka, E., Walaszczyk, A., Chmura, A., Deja, R., Stobiecki, M., Polanski, A., Tarnawski, R., and Widlak, P. (2009) Mass spectrometry-based serum proteome pattern analysis in molecular diagnostics of early stage breast cancer. *J. Transl. Med.* **7,** 60
46. Havel, P. J., Kasim-Karakas, S., Mueller, W., Johnson, P. R., Gingerich, R. L., and Stern, J. S. (1996) Relationship of plasma leptin to plasma insulin and adiposity in normal weight and overweight women: effects of dietary fat content and sustained weight loss. *J. Clin. Endocrinol. Metab.* **81,** 4406–4413
47. Vandeweyer, E., and Hertens, D. (2002) Quantification of glands and fat in breast tissue: an experimental determination. *Ann Anat* **184,** 181–184
48. Tuck, A. B., Chambers, A. F., and Allan, A. L. (2007) Osteopontin overexpression in breast cancer: knowledge gained and possible implications for clinical management. *J. Cell. Biochem.* **102,** 859–868
49. Ribeiro-Silva, A., and Oliveira da Costa, J. P. (2008) Osteopontin expression according to molecular profile of invasive breast cancer: a clinicopathological and immunohistochemical study. *Int. J. Biol. Markers* **23,** 154–160
50. Albert, R., Jeong, H., and Barabasi, A. L. (2000) Error and attack tolerance of complex networks. *Nature* **406,** 378–382
51. Bourbeillon, J., Orchard, S., Benhar, I., Borrebaeck, C., de Daruvar, A., Dubel, S., Frank, R., Gibson, F., Gloriam, D., Haslam, N., Hiltker, T., Humphrey-Smith, I., Hust, M., Juncker, D., Koegl, M., Konthur, Z., Korn, B., Krobitsch, S., Muyldermans, S., Nygren, P. A., Palcy, S., Polic, B., Rodriguez, H., Sawyer, A., Schlapshy, M., Snyder, M., Stoevesandt, O., Taussig, M. J., Templin, M., Uhlen, M., van der Maarel, S., Wingren, C., Hermjakob, H., and Sherman, D. (2010) Minimum information about a protein affinity reagent (MIAPAR). *Nat Biotechnol* **28,** 650–653
52. Uhlén, M., and Hober, S. (2009) Generation and validation of affinity reagents on a proteome-wide level. *J. Mol. Recognition* **22,** 57–64
53. Pla-Roca, M., Leulmi, R. F., Djambazian, H., Sundararajan, S., and Juncker, D. (2010) Addressable nanowell arrays formed using reversibly sealable hybrid elastomer-metal stencils. *Anal. Chem.* **82,** 3848–3855
54. Delamarche, E., Juncker, D., and Schmid, H. (2005) Microfluidics for processing surfaces and miniaturizing biological assays. *Adv. Materials* **17,** 2911–2933
55. Thaxton, C. S., Elghanian, R., Thomas, A. D., Stoeva, S. I., Lee, J.-S., Smith, N. D., Schaeffer, A. J., Klocker, H., Horninger, W., Bartsch, G., and Mirkin, C. A. (2009) Nanoparticle-based bio-barcode assay redefines "undetectable" PSA and biochemical recurrence after radical prostatectomy. *Proc. Natl. Acad. Sci. U. S. A.* **106,** 18437–18442